

3.8 Hydraulic control in a dispersive system: flow over an infinite ridge.

For the most part, our discussion of hydraulics has been limited to cases where the geometry varies gradually in the direction of the channel or coastline. The linear waves permitted, being long in comparison to the lateral dimensions of the flow or conduit, have been nondispersive. Just what happens when this restriction is relaxed is a complex and unsettled matter. The majority of investigations have followed one of two approaches. In the first, the variations of the flow in the along-channel direction are considered long but finite, so that the waves are dispersive but only weakly so. Progress is also facilitated if the nonlinearity is assumed weak, implying that topographic variations must be small. The most interesting behavior occurs when the entire flow is close to a state of hydraulic criticality, so that waves are generated resonantly by the topography. The simplest theory is the one that results in the steady Kd.V. equation for a non-rotating, 1-d flow (Section 1.11). Grimshaw (1987) and others have extended this body of work to include weakly dispersive, hydraulically-driven flows along coastlines. The second approach explores the opposite extreme in which the transverse length scale is essentially infinite. The flows are more idealized but analytically simpler than the nonlinear dispersive models, and waves of all lengths are permitted. The original Rossby adjustment problem (Section 3.1) is an example, though no topography is present. We will focus on another adjustment problem described by Baines and Leonard (1989). Although steady solutions can be readily calculated, the initial-value problem proves quite helpful in developing intuition about the flow. This accounts for the placement of the material in the present chapter on time dependent flows.

Consider an infinite, horizontal plane with a uniform, shallow flow $v^*=v_o^*$, $d^*=d_o^*$, and $u^*=0$. Since the layer depth is uniform, the velocity v_o^* cannot be geostrophically balanced by a tilting free surface or interface. A geostrophic balance requires the presence of a uniform external pressure gradient $\frac{\partial p_o^*}{\partial x^*} = \rho f v_o^*$, perhaps transmitted by an overlying layer.¹ At $t=0$, an isolated, uniform ridge $h=h(y)$ is placed in the path of the flow and the upstream effects in the resulting x^* -independent state are sought.

A fundamental departure from the models considered to this point is the lack of channel side walls and the Kelvin waves they support. Also, because the flow lacks a potential vorticity gradient, Rossby-type waves are absent. This leaves Poincaré (inertia-gravity) waves as the only permissible linear transients and any upstream influence must

¹ For a system with a free surface, the imposed pressure gradient is rather artificial. However, the same governing equation hold if the shallow layer is imagined to be the lower of a two layer system, bounded above by a rigid lid. The pressure gradient is therefore imposed by the rigid lid and gives rise to a geostrophic v in both layers. If the upper layer is much thicker than the lower layer, the single-layer, reduced-gravity, shallow water equations will govern the latter. The reader who wishes to prove this might first consult Section 5.1.

be carried by them. However, we have demonstrated that such waves are inconsequential in establishing the volume transport in the channel adjustment problem (Section 3.1). The transport is generated solely in response to an upstream-propagating Kelvin wave, while the Poincaré wave act to establish the current that crosses the channel at the original position of the barrier. These considerations suggest that the ridge in the present problem will have no influence of the flow far upstream ($y=-\infty$) and that the upstream state can therefore be specified for all time. This assumption is used in the steady theory presented below and is later be tested as part of time-dependent numerical simulations.

The phase and group speeds (in the y^* -direction) of linear Poincaré waves are given in terms of the y^* -wave number l^* by

$$(c^* - v_o^*)^2 = g'd_o^* + \frac{f^2}{l^{*2}} \quad \text{and} \quad (c_g^* - v_o^*)^2 = \frac{(g'd_o^*)^2}{(g'd_o^* + f^2/l^{*2})} \quad (3.8.1a,b)$$

(see Exercise 2). When the wave length is large compared to the deformation radius ($l^*f/(gd_o^*)^{1/2} \ll 1$), $c^* \rightarrow v_o^* \pm f/l^*$ and thus the waves remain dispersive. This behavior contrasts with the long-wave limit of non-dispersion in a coastal or channel geometry. In the opposite limit ($l^*f/(gd_o^*)^{1/2} \gg 1$) rotation becomes unimportant and the phase and group speeds approach the value $v_o^* \pm (g'd_o^*)^{1/2}$. Short waves are therefore nondispersive and are identical to the non-rotating, hydrostatic gravity waves discussed in Chapter 1. The approach flow will be called subcritical, critical, or supercritical with respect to these waves according to $F_o = v_o^*/(g'd_o^*)^{1/2} < 1, = 1, > 1$. Stationary waves ($c^*=0$) can exist if the flow is supercritical and the wave length is given by

$$\lambda^* = 2\pi L_d (F_o^2 - 1)^{1/2}, \quad (3.8.2)$$

where $L_d = (gd_o^*)^{1/2} / f$.

When scaled to the velocity and depth v_o^* and d_o^* of the approach flow, which is now considered fixed in time far upstream of the obstacle, the governing dimensionless shallow water equations become

$$\frac{\partial v}{\partial t} + F_o v \frac{\partial v}{\partial y} + u = -\frac{1}{F_o} \frac{\partial}{\partial y} (d + h), \quad (3.8.3)$$

$$\frac{\partial u}{\partial t} + F_o v \frac{\partial u}{\partial y} - v = -1, \quad (3.8.4)$$

and

$$\frac{\partial d}{\partial t} + F_o \frac{\partial (vd)}{\partial y} = 0. \quad (3.8.5)$$

©Pratt and Whitehead 7/13/06
 very rough draft-not for distribution

The constant factor on the right-hand side of (3.8.4) represents the externally imposed pressure gradient.

If (3.8.3-3.8.5) are linearized about the approach flow $v = 1 + \hat{v}$, $d = 1 + \hat{d}$, with \hat{v}, u , and \hat{d} all $\ll 1$, it can be shown through elementary methods that the steady solution with $(u, \hat{v}, \hat{d}) \rightarrow 0$ as $y \rightarrow -\infty$ is given by

$$\begin{aligned} \hat{d} &= -\frac{h}{1-F_o^2} + \frac{1}{2(1-F_o^2)^{3/2}} \left\{ \int_y^\infty h(\xi) e^{\frac{y-\xi}{(1-F_o^2)^{1/2}}} d\xi + \int_{-\infty}^y h(\xi) e^{\frac{-(y-\xi)}{(1-F_o^2)^{1/2}}} d\xi \right\} \quad (F_o < 1) \\ &= -\frac{h}{1-F_o^2} + \frac{1}{(F_o^2-1)^{3/2}} \int_{-\infty}^y h(\xi) \sin \left[\frac{y-\xi}{(F_o^2-1)^{1/2}} \right] d\xi \quad (F_o > 1) \end{aligned} \quad (3.8.6)$$

The term $-\frac{h}{1-F_o^2}$ is just the linearized hydraulic solution that would exist if the flow were nonrotating and one-dimensional. It predicts that the free surface dips down over the obstacle for subcritical conditions and bulges up over the obstacle for supercritical conditions. However, this is not the whole story when dispersive effects are present. First, it can be seen that the flow is disturbed upstream and/or downstream of the obstacle. This response depends on the Froude number and on the shape of the obstacle. For $F_o < 1$ (Figure 3.8.1a) the flow has upstream/downstream symmetry and the disturbance is felt within a deformation radius of the obstacle. The free surface rises as the obstacle is approached from upstream and the corresponding pressure gradient gives rise to a transverse velocity $u < 0$ in this region. Over the obstacle the free surface descends, then ascends, and these slopes have bands of transverse velocity $u > 0$ and $u < 0$. For $F_o > 1$ there is no disturbance upstream of the obstacle and lee waves with lengths given by (3.8.2) exist downstream (Figure 3.8.1b).

To find steady solutions to the full problem, it is convenient to write the steady versions of (3.8.3-3.8.4) in the form

$$\frac{\partial d}{\partial y} = -\frac{F_o u + \partial h / \partial y}{(1 - F_o^2 / d^3)} \quad (3.8.7)$$

$$\frac{\partial u}{\partial y} = \frac{(1-d)}{F_o} \quad (3.8.8)$$

The steady continuity equation ($vd=1$) has been used to eliminate v in the first relation. The second equation makes use of the statement of uniform potential vorticity: $(1 - F_o du / dy) / d = 1$.

The vanishing of the denominator in (3.8.7) means that

©Pratt and Whitehead 7/13/06
 very rough draft-not for distribution

$$\frac{F_o^2}{d^3} = \frac{F_o^2 v^2}{d} = \frac{v^{*2}}{gd^*} = 1,$$

corresponding to the critical condition for nondispersive Poincaré waves. Again, the corresponding wave lengths are much shorter than L_d . For the critical flow to remain well behaved, (3.8.7) requires that

$$F_o u = -\partial h / \partial y. \quad (3.8.9)$$

In the semigeostrophic case u is asymptotically small and the critical section must occur where $dh/dy=0$. In the present case u may be large enough for the Coriolis acceleration to compete with the horizontal component of the bottom pressure force. Critical flow must occur where the two balance.

Numerical integrations of (3.8.7) and (3.8.8) reveal purely subcritical and supercritical solutions with properties qualitatively similar to the linearized solutions. Examples for a semicircular obstacle are shown in Figures 3.8.2a,c. A third solution exists in which a subcritical-to-supercritical transition occurs over the obstacle (Figure 3.8.2b). Here the upper surface rises as the flow approaches the obstacle, and is then drawn down and through a critical section on the upstream face. The transverse flow at the critical section is negative (into the figure) in accordance with (3.8.9). After its transition to supercritical flow the fluid descends, passes the sill, and a series of lee waves is excited. Lee wave also occur for the other solutions that are supercritical downstream (frames b-e), and are only partially seen in the figures. If the approach flow is supercritical ($F_o > 1$), hydraulically critical states with upstream jumps are possible (frames d and e).

Suppose that one follows a fluid column that originates far upstream in the flow pictured in frame b of the Figure 3.8.2. As the obstacle is approached, the depth increases, the column is stretched, and its vorticity ($\partial u / \partial y$) must become negative in order that its potential vorticity be conserved. A transverse flow in the $-x$ direction is implied and the trajectory of the parcel turns to its left. When the upstream edge of the obstacle is encountered, the depth begins to decrease. The y -velocity v increases to conserve mass and the flow undergoes a transition to a supercritical state. The depth of the column decreases and eventually becomes less than its upstream value, implying a positive ($\partial u / \partial y$). The transverse flow eventually becomes positive ($u > 0$), and the trajectory sweeps back to the right. Downstream of the obstacle, a series of lee waves is encountered, with alternating transverse flows.

Returning now to consideration of the full, time-dependent adjustment problem, it is natural to ask how the solution shown in Figure 3.8.2b is established. Direct numerical integrations of (3.8.3-3.8.5) for $F_o < 1$ show that a bore is excited when the obstacle is sufficiently high (Figure 3.8.3), just as in a channel. The critical obstacle height depends on the topographic shape. As the bore moves upstream the pressure gradient associated with the rapid change in depth sets up a geostrophic transverse velocity. As the pressure gradient becomes increasingly opposed by the Coriolis acceleration, due to the transverse

flow, the bore decays and becomes smooth ($t=4, 12, 20hr$ profiles in Figure 3.8.3). No permanent alteration of the flow occurs more than a distance $\cong L_d$ upstream of the obstacle. The main role of the bore is to establish the transition region in which the approaching flow deepens prior to meeting the upstream edge of the obstacle.

The above model illustrates a number of important departures from hydraulic theory due to wave dispersion. First, the flow away from the obstacle is influenced by the shape of the obstacle, not just its height. Second, lee waves can arise. Both of these features can be expected to arise in other problems when dispersion is present. A more important issue concerns the inability of the obstacle to alter the far upstream flow, regardless of the topographic height. This arises in the present model not so much because of the presence of dispersion, but because to the lack of channel walls. One might ask why the dispersive waves corresponding to the shortest wavelengths cannot alter the flow far upstream. The answer is that while these waves are too short to feel the effects of rotation over a wave period, they do feel rotation over the period (f^{-1}), roughly the time required to move a deformation radius. Rotation in this particular case is also associated with dispersion and thus the upstream influence is limited to a deformation radius from the topography.

Exercises

1. The process of upstream influence due to an obstacle in the nonrotating channel has been described as occurring when the obstacle becomes so high that the upstream energy of the flow is insufficient to allow the flow to climb to the obstacle crest (Section 1.4). In the Baines and Leonard model, the obstacle can apparently be made arbitrarily high without necessitating any change in the upstream conditions. Show why this is possible by first deriving the expression of the Bernoulli function:

$$B(\psi) = F_o \frac{v^2}{2} + \frac{u^2}{2} + F_o^{-1}(d+h) - x(\psi),$$

where $x(\psi)$ is the x -position of the streamline in question. Also note that the flux vd per unit width is constant. As a reminder of the result for a channel, note that the terms involving u and x are absent, and that the maximum possible value of h for a given B is therefore finite. In the present case, however, an arbitrarily large value of h is permissible as it can be compensated for by an equally large $x(\psi)$. Explain this result in physical terms by thinking about the origin of the contribution $x(\psi)$ to the Bernoulli function.

2. Derive the expressions (3.8.1a,b) for the phase and group speeds of the Poincaré waves by altering (2.1.27) to account for the presence of a mean flow $v^*=v_o^*$ and then specializing to the case of independence on the transverse coordinate x^* .

©Pratt and Whitehead 7/13/06
very rough draft-not for distribution

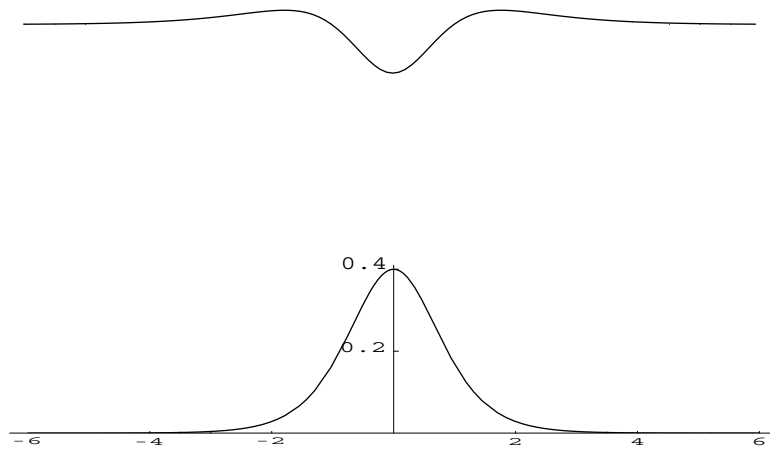
3. Derive the equations governing the shape of nonlinear lee waves over a horizontal bottom in the context of the above model. (See *Baines and Leonard 1989 for a solution*).

Figure Captions

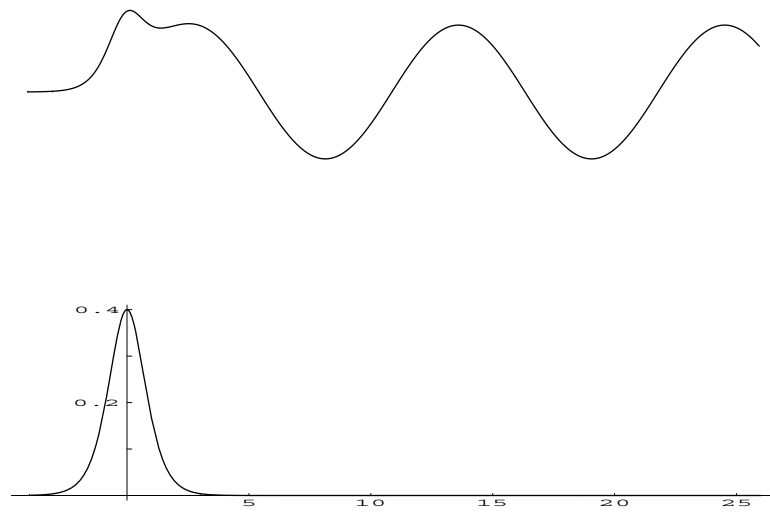
3.8.1 Sketches of linear solutions based on (3.8.6) for (a) $F_o=0.5$ and (b) $F_o=2.0$, both with $h(y)=0.3\text{sech}^2(y)$. [Based on a figure from Baines and Leonard, 1989]

3.8.2 Possible steady, nonlinear solutions for flow over a semi-circular obstacle. The length of the obstacle is (a) purely subcritical flow; (b) subcritical approach flow ($F_o < 1$) with a hydraulic transition on the upstream face of the obstacle; (c) purely supercritical flow; (d and e) supercritical approach flow ($F_o < 1$) with a stationary jump upstream of the obstacle and a hydraulic transition over the obstacle. Lee waves exist in cases (b)-(e). [Figure 5 of Baines and Leonard (1989).]

3.8.3 Evolution of the free surface as a result of adjustment to the introduction of a semi-infinite obstacle (shaded region), with $F_o=.85$ and $h_m^*/d_o^*=.667$. The curve in the upper frame shows the transverse velocity at 20hrs, while the lower set of curves shows the free surface at various times. [Based on Figure 3 of Baines and Leonard (1989).]



(a)



(b)

Fig. 3.8.1

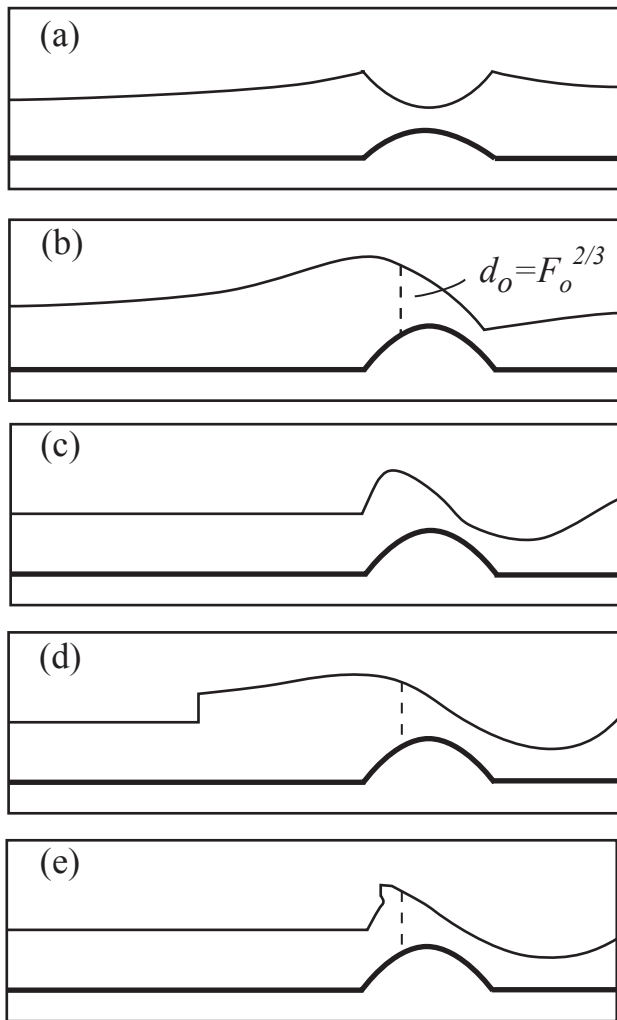


Fig. 3.8.2

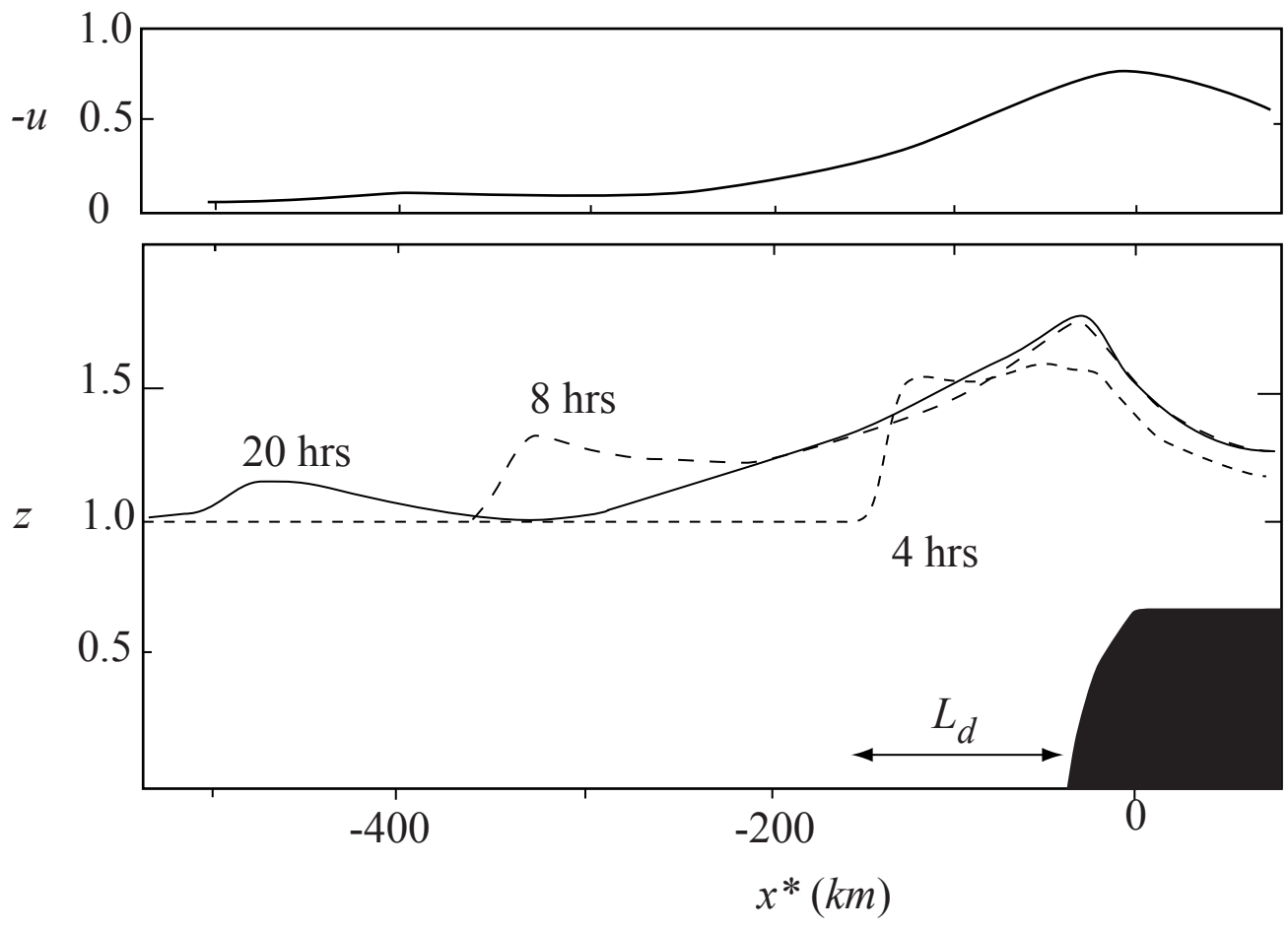


Figure 3.8.3